Identification of cancer-associated fibroblast biomarkers in cutaneous squamous cell carcinoma

YUANYUAN DENG[1], JUE QI[1], YU TANG[2], YUETING CUN[3], QIAN HE[4] and LI HE[1]

[1]Department of Dermatology, First Affiliated Hospital of Kunming Medical University, Kunming, Yunnan 650032, P.R. China;
[2]Yunnan Key Laboratory of Breast Cancer Precision Medicine, Yunnan Cancer Hospital, The Third Affiliated Hospital of Kunming Medical University, Peking University Cancer Hospital, Kunming, Yunnan 650118, P.R. China;
[3]Department of Dermatology, Chuxiong People's Hospital, Chuxiong, Yunnan 675000, P.R. China;
[4]Institute of Biomedical Engineering of Kunming Medical University, Kunming, Yunnan 650032, P.R. China

Received July 3, 2026; Accepted August 12, 2026

DOI: 10.3892/ol.2026.15869

Abstract. Cancer-associated fibroblasts (CAFs) are a key component of the tumor microenvironment and serve key roles in tumor progression, extracellular matrix remodeling and immune modulation. Nevertheless, no consensus has been reached thus far on biomarkers for CAFs in cutaneous squamous cell carcinoma (cSCC), a situation that hinders mechanistic research into this disease. In the present study, large-scale datasets were used to independently screen for candidate CAF biomarkers and subsequently validate their authenticity at the tissue level in cSCC specimens, including those derived from actinic keratosis (AK). Microarray datasets (GSE139505 and GSE191334) from the Gene Expression Omnibus database were analyzed to identify differentially expressed genes (DEGs) in cSCC tissues compared with normal skin tissues. These DEGs were then intersected with cSCC-associated genes retrieved from GeneCards and a set of 50 previously identified CAF marker genes. The expression of candidate genes was further validated in cSCC tissue samples and normal skin samples by immunohistochemistry. To gain further insight into the changes of these candidate genes across different stages of cSCC progression, AK samples were also incorporated during validation using multiplex immunofluorescence technology. Enrichment analysis revealed that the overlapping genes were primarily involved in the MAPK signaling pathway, PI3K-Akt signaling pathway and extracellular matrix organization. A total of five genes, melanoma cell adhesion molecule (MCAM), actin α2, smooth muscle (ACTA2), transgelin (TAGLN), platelet derived growth factor receptor β (PDGFRB) and regulator of G protein signaling 5 (RGS5), were revealed to be significantly upregulated in cSCC compared with normal skin. Among these, MCAM stood out from the cross-analysis pipeline, whereas ACTA2, TAGLN, RGS5 and *PDGFRB* were CAF markers identified based on single-cell literature studies. The five genes (MCAM, ACTA2, TAGLN, PDGFRB and RGS5), can serve as candidate biomarkers for CAFs, facilitating their identification and definition. This provides a useful reference for further investigation into the contribution of CAF in the progression of cSCC.

Correspondence to: Professor Li He, Department of Dermatology, First Affiliated Hospital of Kunming Medical University, 295 Xichang Road, Kunming, Yunnan 650032, P.R. China
E-mail: drheli2662@126.com; heli1@ydyy.cn

Key words: cutaneous squamous cell carcinoma, cancer-associated fibroblasts, biomarkers, bioinformatics

Introduction

Cutaneous squamous cell carcinoma (cSCC), originating from epidermal keratinocytes, is the second most common tumor in humans (1). The estimated lifetime incidence of cSCC is between 7 and 11%, although its incidence has been rising in recent years. In addition to cosmetic concerns, advanced cSCC poses a notable risk of mortality (2,3). A previous study has shown that the metastasis risk for patients with cSCC is 3.7%, and the disease-specific mortality risk is 2.1% (3). Tumor diameter of ≥2 cm, invasion beyond fat, poor differentiation, perineural invasion and location on the ear, temple or anogenital area are risk factors associated with poor prognosis (3). Molecular targeted therapy has emerged as a promising treatment for cSCC (4,5), offering new hope to patients. However, cSCC often exhibits variable responses to targeted therapies (4,6), contributing to worse prognosis. Several molecular targets have been identified in cSCC, including the EGFR pathway, the Hedgehog pathway and the MAPK pathway (7). Clinical trials targeting these pathways have shown promising results (8-11). Upregulation of EGFR, observed in 35 to 56% of cSCC cases, leads to increased cell proliferation and survival (12-14). EGFR activation triggers signaling cascades, including the MAPK and PI3K/Akt pathways, promoting cell proliferation and inhibiting apoptosis (15). Uncontrolled EGFR signaling in cSCC drives uncontrolled cell proliferation and resistance to apoptosis, contributing to tumor growth and spread. Cetuximab and erlotinib effectively treat advanced cSCC by inhibiting EGFR, which is frequently upregulated in

cSCC tumors (16). Most current treatment strategies target isolated pathways within cSCC, with limited consideration of the complex interactions between tumor cells and their microenvironment. Although studies have focused on immune cells and vascular endothelial cells within the cSCC microenvironment (1,17), there is limited research on whether cancer-associated fibroblasts (CAFs) serve a key role in the tumor stroma. While some studies have identified CAF marker-expressing cells in cSCC (18-21), they have not comprehensively described the impact of CAFs on cSCC and its microenvironment. Importantly, previous research has often relied on cell surface markers; however, the surface markers for subpopulations have not yet been standardized, which has introduced complexity to subsequent research.

To address this gap, an independent prioritization was performed using bulk datasets and intersection with GeneCards. In addition, tissue-level validation of selected CAF-associated markers and observational multiplex immunofluorescence (mIF) assessment were conducted across normal skin (NL), actinic keratosis (AK) and cSCC samples. The genes identified in the present study facilitate the recognition of tumor-associated fibroblasts and enhance understanding of their roles and molecular mechanisms in cSCC carcinogenesis and progression.

Materials and methods

Microarray data. GEO (http://www.ncbi.nlm.nih.gov/geo) (22) is a publicly accessible repository for functional genomics data, including high-throughput gene expression profiles from chips and microarrays. The GSE191334 (GPL11154) (23,24) and GSE139505 (GPL18573) (24) datasets, were retrieved from the GEO. Probe identifiers were converted to official gene symbols using platform-specific annotation files. The GSE191334 dataset comprised 7 cSCC tissues and 7 non-cancerous controls, while the GSE139505 dataset included 9 cSCC samples and 7 non-cancerous controls. Additionally, cSCC-related genes were identified using the GeneCards database (https://www.genecards.or) (25). During the gene screening process, the advanced search function was not enabled and only a basic keyword search on the GeneCards homepage was performed. By entering the keyword 'cutaneous squamous cell carcinoma', a gene list containing 6,422 genes was obtained (retrieved on October 23, 2024).

Identification of DEGs. DEGs between cSCC and non-cancerous samples were identified using GEO2R (http://www.ncbi.nlm.nih.gov/geo/geo2r), an interactive web-based tool for comparing gene expression across experimental conditions. To balance the identification of statistically significant genes and control false positives, P-values adjusted by the Benjamini-Hochberg false discovery rate (FDR) were used. Probes lacking gene symbols were excluded, and those mapping to the same gene were averaged. Given the use of bulk sequencing data, genes with |log fold change|≥1 and an adjusted P<0.05 were considered statistically significant to capture biologically relevant changes.

To obtain robust and reproducible cSCC-related candidate genes, the intersection of DEGs screened from the two datasets as target hub genes were extracted. Cross-dataset batch correction and DEG meta-analysis were not implemented in this workflow: Raw expression data from two cohorts were never integrated, eliminating inter-dataset batch interference; the intersection filtering strategy was prioritized over meta-analysis to screen genes with consistent differential expression trends in two independent sample batches.

Kyoto encyclopedia of genes and genomes (KEGG) and gene ontology (GO) enrichment analyses. Functional annotation of DEGs was performed using the Database for Annotation, Visualization and Integrated Discovery (DAVID) bioinformatics resource (http://david.ncifcrf.gov; version 2021) (26), which offers integrated biological data and tools for gene functional annotation. KEGG (27) and GO (28) analyses were conducted to uncover high-level functional and pathway-related insights. To avoid false positive outcomes induced by multiple simultaneous tests of numerous gene sets, Benjamini-Hochberg FDR multiple testing correction was applied for all enrichment results. Terms with FDR <0.05 were considered statistically significant.

PPI network construction and module analysis. PPI networks were generated using STRING (http://string-db.org; version 12.0) (29). Interactions with a combined score >0.4 were deemed significant. The resulting networks were visualized and analyzed in Cytoscape (version 3.10.2) (30). Dense network modules were identified using the MCODE plugin (version 2.0.3) (31) with the following parameters: MCODE score >5, degree cut-off=2, node score cut-off=0.2, max depth=100 and k-score=2. Functional enrichment of genes within the key module was further assessed via KEGG and GO using DAVID.

Hub-protein identification. Network topology was evaluated using CytoHubba (version 0.1) (32) to identify hub proteins. Both local [degree, maximum clique centrality (MCC), maximum neighborhood component and density of maximum neighborhood component] and global (edge percolated component, bottleneck, eccentricity, closeness, radiality, betweenness and stress) ranking methods were applied. Hub proteins were determined based on the MCC scores, focusing on the top 10 nodes.

IHC staining. After ethical approval, between September 2020 and March 2024, samples were collected from 53 patients (18 men and 35 women; median age, 62 years; range 47-72 years) in the outpatient operating room of the Department of Dermatology at the First Affiliated Hospital of Kunming Medical University (Kunming, China). These samples included 21 normal skin specimens and 32 skin specimens diagnosed as cSCC.

The inclusion criteria were as follows: i) Voluntary participation in the present study, consent for the collected samples to be used for scientific research and publication in public journals, and signed informed consent forms; and ii) normal skin or cSCC lesions located on sun-exposed areas of the face and neck. The exclusion criteria were as follows: i) Severe systemic diseases or other non-squamous cell neoplasms; ii) patients who had undergone liver, kidney or bone marrow transplantation; iii) systemic use of glucocorticoids, immunosuppressants,

radiotherapy or chemotherapy within 1 month, or topical treatment of local skin lesions within 1 week; iv) patients with long-term exposure to carcinogenic substances such as radiation, asphalt, coal tar or xylene, or those with squamous cell carcinoma secondary to trauma, scarring, viral warts or chronic ulcers; and v) patients with psychiatric disorders.

Formalin-fixed, paraffin-embedded tissue sections (4 μm) were baked at 65˚C for 2 h, deparaffinized and rehydrated through a graded alcohol series. Specifically, xylene I and xylene II were applied for 10 min each at room temperature, and 100, 95, 80 and 70% ethanol were applied for 5 min each at room temperature. Antigen retrieval was performed by heating sections in 10 mM citrate buffer (pH 6.0) using a microwave. Endogenous peroxidase activity was blocked with peroxidase blocking solution (3% H_2O_2, at room temperature) for 10 min, followed by incubation with 10% normal goat serum (cat. no. ab138478; Abcam) for 1 h to minimize non-specific binding. Sections were then incubated overnight at 4˚C with primary antibodies against MCAM (1:250; cat. no. ab75769; Abcam), ACTA2 (1:100; cat. no. ab7817; Abcam), TAGLN (1:200; cat. no. ab213273; Abcam), RGS5 (1:200; cat. no. ab314671; Abcam) and PDGFRB (1:100; cat. no. ab313777; Abcam). After washing, slides were treated with an IHC enhancer for 20 min and incubated with an HRP-conjugated secondary antibodies (1:200; cat. nos. A0208 and A0192; Beyotime Biotechnology) at 37˚C for 1 h. Detection was performed using DAB, and sections were counterstained with hematoxylin, dehydrated, cleared and mounted. Whole-slide digital images of histological sections were acquired using CaseViewer software (V2.4.0.119028; 3DHISTECH, Ltd.). Images at x40 objective magnification were exported, and the corresponding scale bar length for this magnification was 20 μm. All quantitative morphological analyses were performed with reference to the 20 μm scale standard. IHC results were evaluated using the H-score semiquantitative scoring method (33,34). H-score was calculated as the product of the staining intensity score (0-3) and positive cell percentage score (0-4). Intensity: 0: colorless; 1: light yellow; 2: brownish yellow; and 3: tan. Percentage score: 0, 0-5%; 1, 6-25%; 2, 26-50%; 3, 51-75%; and 4, 76-100%. For each sample, five random non-overlapping high-power fields (x40) were evaluated. The final H-score per sample was the mean of the five fields, ranging from 0 to 12. All IHC slides were independently evaluated by two experienced dermatopathologists in a double-blinded manner to reduce subjective scoring bias, and group data are reported as mean ± SD.

mIF

Antibodies and reagents. The following primary antibodies were used: Rabbit monoclonal anti-ACTA2 (1:250; cat. no. ab124964; Abcam) and rabbit polyclonal anti-TAGLN (1:250; cat. no. ab14106; Abcam). As both primary antibodies were raised in the same host species (rabbit), tyramide signal amplification (TSA) was employed for sequential detection without cross-reactivity. The secondary antibody was HRP-conjugated goat anti-rabbit IgG (1:1,000; cat. no. ab6721; Abcam). TSA substrates were Cy3-tyramide (for ACTA2, red channel) and AF488-tyramide (for TAGLN, green channel). Nuclei were counterstained with DAPI (blue channel).

Tissue samples. Between January 2024 and May 2024, samples were collected from sun-exposed areas of the face and neck of 18 patients (7 men and 11 women; median age 65 years; range 49-80 years) in the outpatient operating room of the Department of Dermatology at the First Affiliated Hospital of Kunming Medical University. These samples included 6 normal skin specimens, 6 specimens diagnosed as AK and 6 specimens diagnosed as cSCC.

Multiplex staining procedure. Tissue sections were deparaffinized, rehydrated and subjected to heat-induced antigen retrieval (same method as aforementioned). Permeabilization was performed with 0.5% Triton X-100 in PBST, followed by blocking with 10% goat serum (at room temperature, 1 h).

i) Round 1 (ACTA2). Sections were incubated overnight at 4˚C with the anti-ACTA2 antibody. After washing, they were incubated with the HRP-conjugated secondary antibody for 30 min, followed by Cy3-tyramide (1:500) for 10 min in the dark.

For antibody stripping, to remove non-covalently bound antibody complexes, slides were subjected to a second round of antigen retrieval (identical conditions as the first retrieval). After naturally cooling to room temperature, the sections were washed three times with PBS for 5 min each, the tissue was ready for the next round.

ii) Round 2 (TAGLN). Slides were re-blocked and incubated with the anti-TAGLN antibody overnight at 4˚C. After washing, slides were incubated with the same HRP-conjugated secondary antibody (1:1,000; 30 min; at room temperature), followed by AF488-tyramide (1:200 in amplification buffer) for 10 min in the dark.

iii) Nuclear counterstaining and mounting. DAPI solution (1 μg/ml in PBS) was applied for 10 min at room temperature. Slides were briefly rinsed in distilled water, air-dried and mounted with an anti-fade mounting medium, then stored at 4˚C until imaging.

Image acquisition and quantification. mIF images were acquired using a Pannoramic MIDI II whole-slide scanner (3DHISTECH Ltd.). The following fluorescence channels were used: DAPI (excitation, 358 nm; emission: 461 nm, blue channel), AF488 (excitation, 495 nm; emission, 519 nm; green channel for TAGLN) and Cy3 (excitation: 550 nm; emission: 570 nm; red channel for ACTA2). Image visualization was performed using CaseViewer (version 2.4.0) software. Fluorescence images from the red channel (ACTA2) and green channel (TAGLN) were merged using CaseViewer software. Co-localization of ACTA2 and TAGLN appeared as yellow in the merged images. For each section, five random fields were captured at x40 magnification. The absolute number of $ACTA2^{+}TAGLN^{+}$ double-positive cells per high-power field (x40) was quantified.

Statistical analysis. Statistical analyses were performed using GraphPad Prism (version 9.5.1; Dotmatics). The IHC H-score data from each group were first subjected to the Kolmogorov-Smirnov normality test. If the test result was $P>0.05$, the data were considered to follow a normal distribution, and comparisons between two groups were performed using an independent samples t-test. If the test result was $P\leq0.05$, the data were considered not to follow a normal

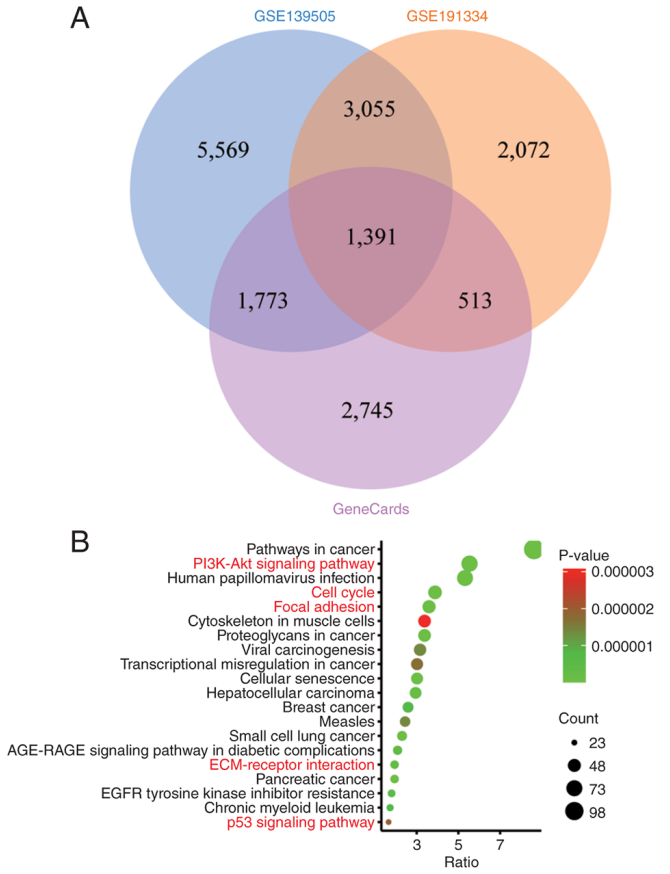


Figure 1. Overlapping genes among three sets and their functional enrichment. (A) Venn diagram of two Gene Expression Omnibus datasets and one GeneCards dataset. (B) Kyoto Encyclopedia of Genes and Genomes enrichment analysis of differentially expressed genes. ECM, extracellular matrix; AGE-RAGE, advanced glycation end-products-receptor for advanced glycation end-products.

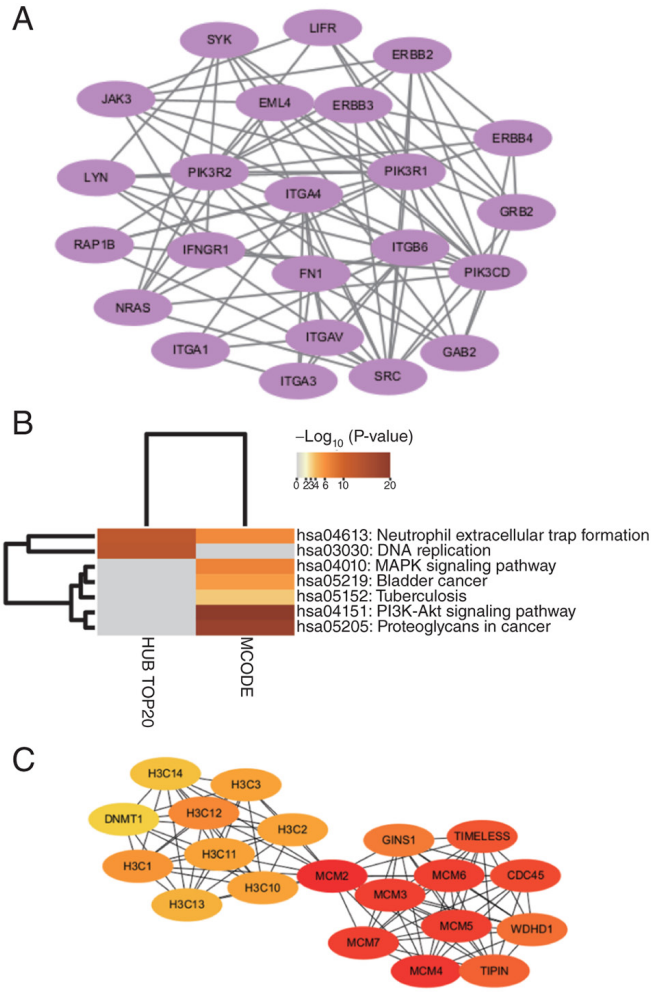


Figure 2. PPI network analysis results. (A) Display of MCODE analysis module genes. (B) Kyoto Encyclopedia of Genes and Genomes enrichment analysis of MCODE module genes and CytoHubba MCC TOP 20 genes. (C) Display of CytoHubba Maximum Clique Centrality Top 20 genes.

distribution, and comparisons between two groups were performed using the Mann-Whitney U test. All data in the present study were normally distributed, and a $P<0.05$ was considered to indicate a statistically significant difference.

Results

Identification of DEGs in cSCC. Standardized analysis of the two microarray datasets identified DEGs (11,788 in GSE139505 and 7,031 in GSE191334), intersecting with the 6,422 cSCC-related genes in GeneCards, yielding 1,391 genes (Fig. 1A).

KEGG and GO enrichment analysis of DEGs. To investigate biological processes in cSCC, pathway enrichment analysis was conducted using DAVID. GO analysis of DEGs revealed significant enrichment in biological processes related to cell proliferation, angiogenesis and ECM (Fig. S1). Cellular component enrichment highlighted cytoplasmic, nuclear and ECM changes. Molecular function analysis indicated enrichment in protein binding, ATP binding, DNA binding, cytoskeletal components and ECM. KEGG pathway analysis indicated enrichment in the 'PI3K-Akt signaling pathway', 'cell cycle', 'focal adhesion', 'ECM-receptor interaction' and the 'p53 signaling pathway' (Fig. 1B).

PPI network construction and module analysis. The PPI network of DEGs (Table SI) was constructed, and critical modules were identified using Cytoscape (Fig. 2A). Functional analysis of module genes indicated enrichment in MAPK, PI3K-Akt and ECM pathways (Fig. 2B). Further analysis with the Cytoscape Cytohubba plugin identified the top 20 genes by MCC score, emphasizing genes involved in DNA replication (Fig. 2C), suggesting bulk sequencing may reflect tumor cell biology, with microenvironmental changes less prominent in bulk data.

Analysis and identification of candidate CAF biomarkers. Reviewing single-cell studies in PubMed and Google Scholar, 50 reported CAF marker genes in cSCC were identified (Table I; Fig. 3A) (18-21). Cross-referencing these with the 1,391 DEGs yielded 20 overlapping genes (Fig. 3A), including CXCL13, COL1A1, FN1, WNT5A, MYH11, MCAM, TGFB1, STMN1, MMP11, COL3A1, LUM, TNC, OGN, FAP, TGFB3, TOP2A, COL4A1, MKI67, COL6A3 and DCN. Further IHC validation revealed higher expression of *MCAM* in cSCC compared with NL (Figs. 3B and S2A). Genes frequently identified in single-cell studies but not in bulk sequencing, such as

Table I. Fibroblast marker genes summarized in single-cell cutaneous squamous cell carcinoma studies.

Cluster	Markers	Annotation	(Refs.)
Fib1	RGS5, KCNJ8, ACTA2 and MCA	Angiogenesis	(18)
Fib2	COL1A1/2, LUM and DC	Classic fibroblasts	(18)
Fib3	ACTA2, MYH11 and AOC3	Myofibroblasts	(18)
Fib4	MGST1, MFAP5, WISP2 and PTGDS	Reticular fibroblasts	(18)
Fib5	ASPN, OGN and TNN	Mesenchymal fibroblasts	(18)
Fib6	STMN1, MKI67 and TOP2A	Proliferating fibroblasts	(18)
CAFs	LRP1, SDC1, TFPI, FN1, THBS1, TGFB1 and TGFB3	-	(19)
mCAFs	RGS5, DCN, COL6A2, COL1A1, COL1A2	-	(21)
iCAFs	DCN, COL6A2, COL1A1, COL1A2	-	(21)
IL7R$^+$ CAFs	IL7R, IL1B, IL6, CXCL1, CXCL3, CXCL5, CXCL6, CXCL8, CXCL13, CXCL14, DCN, COL6A2, COL1A1, COL1A2, COL4A1, COL6A1, COL6A2, COL6A3, FN1, TNC and THY1	Tumor recurrence	(21)
CAFs	ACTA2, FAP	-	(20)
iCAF	COL6A2, COL6A3, FN1, TNC and THY1	-	(20)
myCAF	COL3A1, C3, IGF1, ADM, CXCL12, COL3A1, MMP11, WNT5A and ANGPTL2	-	(20)

Fib, fibroblast; CAFs, cancer-associated fibroblasts; myCAF, myofibroblastic cancer-associated fibroblast; iCAF, inflammatory cancer-associated fibroblast; mCAF, matrix cancer-associated fibroblast; RGS5, regulator of G protein signaling 5; KCNJ8, potassium inwardly rectifying channel subfamily J member 8; ACTA2, actin α2, smooth muscle; MCAM, melanoma cell adhesion molecule; TAGLN, transgelin; PDGFRB, platelet derived growth factor receptor β; LUM, lumican; DCN, decorin; MYH11, myosin heavy chain 11; AOC3, amine oxidase copper containing 3; MGST1, microsomal glutathione S-transferase 1; MFAP5, microfibril associated protein 5; WISP2, WNT1 inducible signaling pathway protein 2; PTGDS, prostaglandin D2 synthase; ASPN, asporin; OGN, osteoglycin; TNN, tenascin N; STMN1, stathmin 1; MKI67, marker of proliferation Ki-67; TOP2A, DNA topoisomerase II α; LRP1, LDL receptor related protein 1; SDC1, syndecan 1; TFPI, tissue factor pathway inhibitor; FN1, fibronectin; THBS1, thrombospondin 1; CXCL, C-X-C motif chemokine ligand; FAP, fibroblast activation protein; IGF1, insulin growth factor 1; C3, complement C3; ADM, adrenomedullin; THY1, Thy-1 cell surface antigen; ANGPTL2, angiopoietin like-2; TNC, tenascin C.

ACTA2, TAGLN, RGS5 and PDGFRB, also displayed elevated expression in cSCC compared with NL (Figs. 3C and S2B), highlighting the utility of single-cell technology in uncovering complex biological variations within tumors. Meanwhile, mIF also demonstrated the presence of a CAF subset co-expressing the genes ACTA2 and TAGLN throughout the pathological evolution of human skin tissue from the normal state to cSCC (Fig. 3D). In normal samples, double-positive cells had been relatively scarce.

Discussion

cSCC is a common epithelial malignancy with an estimated lifetime incidence of 6 to 11% (35-37) and AK has been considered its precancerous lesion. Up to 5% of cSCC cases progress to metastatic cSCC, and this rate is higher in types of cancer with multiple high-risk factors. It has been reported that male sex, advanced age and immunocompromised status are associated with a higher risk of metastasis (38). Advanced cSCC is often fatal. cSCC typically exhibits a high tumor mutational burden (39-41), driven by an accumulation of risk genes, primarily induced by UV radiation (42), as well as interactions with the stroma and local immune modulation, which collectively drive tumor progression (43-45). AK is a precancerous lesion of cSCC (46,47), with ~10% of AK cases progressing to cSCC within 2 years (48). Although multiple risk factors have been identified, cumulative UV exposure with advancing age remains the greatest risk factor, particularly on sun-exposed areas of the face and neck. As a prototypic keratinocyte carcinoma, cSCC arises through a stepwise progression from healthy epidermal keratinocytes to precancerous lesions and subsequent cSCC, involving cumulative mutations in pathways that regulate cell division, communication, apoptosis and differentiation, along with abnormal interactions with the tumor microenvironment (TME) and immune surveillance (49-52). These findings deepen the understanding of the complex mechanisms underlying cSCC pathogenesis. In the present study, two cSCC datasets were integrated from the GEO database and cSCC-related genes from GeneCards, along with previously reported CAF marker genes in cSCC from PubMed and Google Scholar, as well as IHC and mIF data under different pathological conditions. The candidate genes identified in the present study facilitate recognition of tumor-associated fibroblasts and provide insights into their potential role and molecular mechanisms in cSCC carcinogenesis and progression. Moreover, the present study emphasizes the necessity of further exploration into cellular heterogeneity and intercellular interactions within cSCC, aspects that will be investigated in subsequent studies.

During tumor formation, progression and dissemination, cancer cells interact with diverse cell types within the

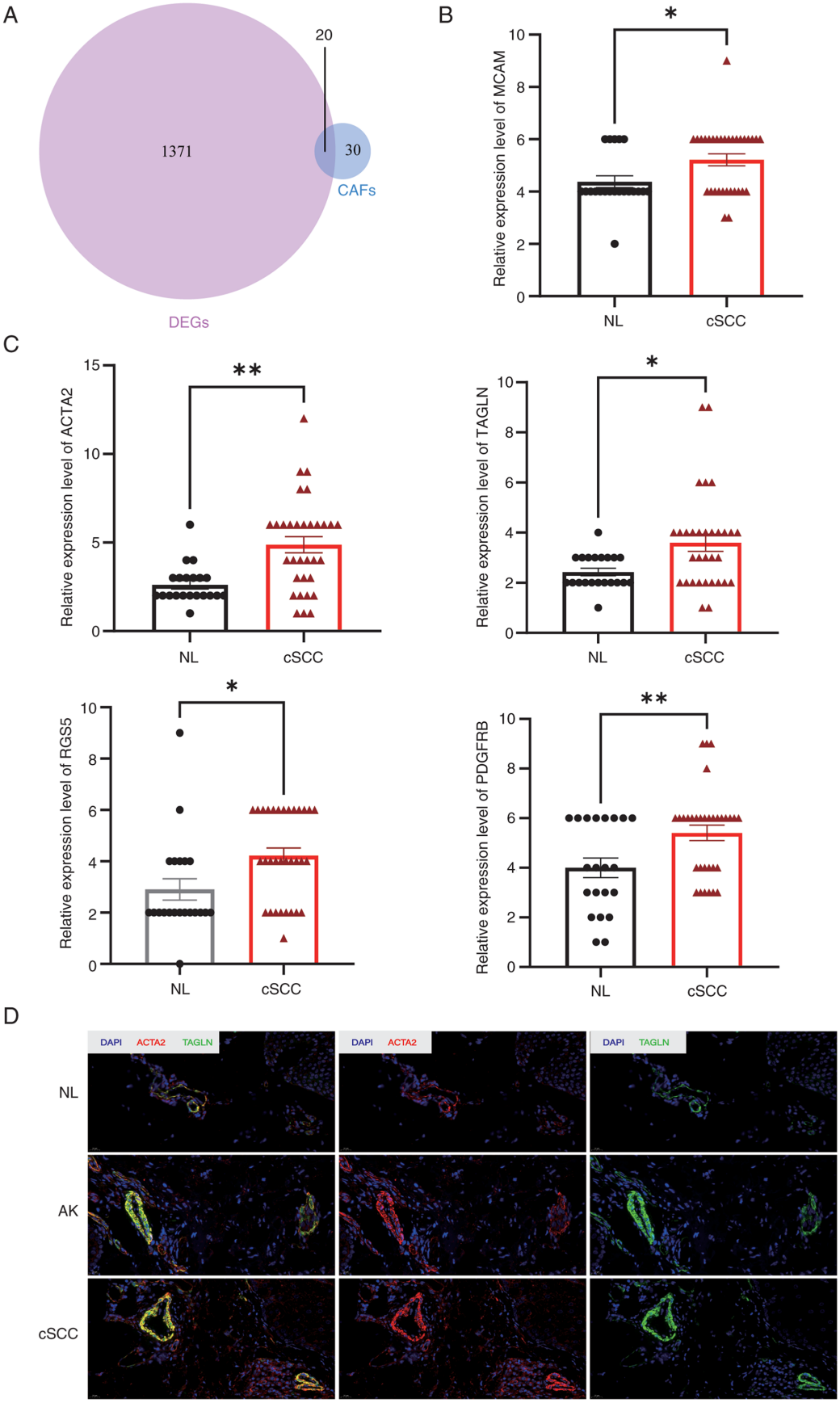


Figure 3. Candidate gene identification. (A) Intersection of DEGs and CAFs from the cSCC single-cell study. (B) Immunohistochemical analysis statistics of MCAM in cSCC and normal samples. (C) Immunohistochemical analysis statistics of ACTA2, TAGLN, RGS5 and PDGFRB in cSCC and NL. *P<0.05 and **P<0.01. (D) Results of multiplex immunofluorescence for NL, AK and cSCC. Magnification, x40. CAFs, cancer-associated fibroblast markers; cSCC, cutaneous squamous cell carcinoma; NL, normal skin; AK, actinic keratosis; MCAM, melanoma cell adhesion molecule; of ACTA2, actin α2 smooth muscle; TAGLN, transgelin; RGS5, regulator of G protein signaling 5 and PDGFRB, platelet derived growth factor receptor β; DEGs, differentially expressed genes.

surrounding stroma, forming the TME, which is key to disease progression (53). The TME is marked by high concentrations of CAFs, which support tumor advancement by remodeling the surrounding ECM and secreting various factors that promote tumorigenesis (18,54,55). The advent and standardization of single-cell transcriptomics has now enabled comprehensive study of various cell types, including CAFs, as well as CAF heterogeneity across different tumor types (18,54,55). Notably, the subpopulations identified in various studies, even within the same disease type, do not consistently align, including the marker genes (18-21). The present study revealed that MCAM not only demonstrated high gene expression in bulk sequencing data, but was also validated by IHC. MCAM serves a role in cell adhesion and cohesion within endothelial monolayers at vascular and tissue intercellular junctions. It is highly expressed across various types of cancer (56-58). In colorectal cancer, $MCAM^+$ fibroblasts interact with IL-1 receptor 1, enhancing NF-κB/IL-34/C-C motif chemokine ligand 8 signaling to recruit macrophages and form a pro-TME (59). The role and mechanism of MCAM within the cSCC TME warrants further investigation.

Certain genes, identified as CAF markers in multiple single-cell cSCC studies (Table I) (18-21), were not among the DEGs identified in bulk sequencing data, but demonstrated their high expression in cSCC through IHC. This highlights the advantage of single-cell techniques in exploring complex biological changes within tumors. For example, the gene ACTA2 is a known marker of myofibroblasts in cSCC and oral squamous cell carcinoma and is associated with worse prognosis (18,60). In glioblastoma, it marks mature CAFs (61), while in colorectal cancer, $ACTA2^+$ fibroblasts can induce immunosuppression (59). The gene TAGLN has been reported as upregulated across various tumors. For instance, this gene mediates ECM stiffness in ovarian cancer progression through the Ras homolog family member A/Rho-associated protein kinase pathway (62), enhances stem cell characteristics in head and neck squamous cell carcinoma via the TGFBI-TAGLN axis (63) and promotes the hypoxic response and maintenance of glioblastoma stem cells through p53 acetylation (64). In the present study, the mIF results revealed the presence of $ACTA2^+TAGLN^+$ cell subsets in all AK and cSCC samples. However, their contribution to cSCC progression requires further functional and mechanistic studies.

The gene RGS5 is implicated in angiogenesis across various tumors (65). In liver cancer, it mediates Wnt/β-catenin signaling for tumor progression (66), and in triple-negative breast cancer, it is a marker of extracellular matrix CAFs, potentially serving a role in metabolic pathways (67,68). In breast cancer, a CAF subset expressing integrin α11 and PDGFRβ promotes tumor invasion via PDGFRβ/JNK signaling and tenascin C upregulation, and targeting this axis suppresses CAF-induced invasiveness (67). In the present study, IHC further validated that these genes show a trend toward higher expression in cSCC.

Leveraging large-scale bulk transcriptomic datasets, GeneCards-based cross-analysis and multi-tissue validation, the present study identified a panel of candidate genes of CAF in cSCC, namely MCAM, ACTA2, TAGLN, RGS5 and PDGFRB, with a particular focus on the $ACTA2^+TAGLN^+$ CAF subpopulation. These observations establish a foundation for unraveling the contributions of CAFs to cSCC biology. Nonetheless, the present study has certain limitations that merit consideration. The mIF assessment, although informative, was constrained by a modest sample size (six paired samples), which may limit extrapolation to broader patient populations. Furthermore, the approach does not permit causal inference regarding the functional impact of the identified genes on CAF behavior or tumor progression. Additionally, the study was conducted at a single time point, precluding analysis of the temporal dynamics of CAF activation and plasticity during cSCC evolution. To overcome these limitations, future investigations will incorporate single-cell transcriptomic profiling to resolve CAF heterogeneity at the single-cell level, followed by functional characterization, including gain- and loss-of-function assays, lineage tracing and co-culture models, to delineate the precise mechanisms by which $ACTA2^+TAGLN^+$ CAFs influence tumor invasion, immune evasion and even therapeutic resistance. Ultimately, such endeavors may inform the rational design of CAF-targeted interventions for cSCC.

Acknowledgements

Not applicable.

Funding

The present work was supported by the National Natural Science Foundation of China (grant no. 82260517).

Availability of data and materials

The data generated in the present study may be requested from the corresponding author.

Authors' contributions

YD contributed to conceptualization, visualization, and the writing and revision of the original draft. JQ, YC and QH made substantial contributions to the acquisition, analysis and interpretation of data, including the collection of human tissue samples, as well as the preparation, staining and reading of pathology slides. YT contributed to conceptualization. LH contributed to conceptualization, resources, funding acquisition, supervision, and the review and editing of the manuscript. All authors read and approved the final version of the manuscript. YD and LH confirm the authenticity of all the raw data.

Ethics approval and consent to participate

The present study protocol was approved by the Ethics Committee of the First Affiliated Hospital of Kunming Medical University [approval no. (2020)-L-29], and written informed consent was obtained from all patients. All procedures performed in the present study involving human participants were in accordance with the Declaration of Helsinki (as revised in 2013).

Patient consent for publication

Not applicable.

Competing interests

The authors declare that they have no competing interests.

References

1. Chang MS, Azin M and Demehri S: Cutaneous squamous cell carcinoma: The frontier of cancer immunoprevention. Annu Rev Pathol 17: 101-119, 2022.
2. Karia PS, Han J and Schmults CD: Cutaneous squamous cell carcinoma: Estimated incidence of disease, nodal metastasis, and deaths from disease in the United States, 2012. J Am Acad Dermatol 68: 957-966, 2013.
3. Schmults CD, Karia PS, Carter JB, Han J and Qureshi AA: Factors predictive of recurrence and death from cutaneous squamous cell carcinoma: A 10-year, single-institution cohort study. JAMA Dermatol 149: 541-547, 2013.
4. Hughes BGM, Munoz-Couselo E, Mortier L, Bratland Å, Gutzmer R, Roshdy O, González Mendoza R, Schachter J, Arance A, Grange F, *et al*: Pembrolizumab for locally advanced and recurrent/metastatic cutaneous squamous cell carcinoma (KEYNOTE-629 study): An open-label, nonrandomized, multicenter, phase II trial. Ann Oncol 32: 1276-1285, 2021.
5. Hiller A, Oxford M, Kulkarni P, Fornadley J, Lo A, Sivik J, Drabick J and Vakharia K: Efficacy of cemiplimab as adjuvant or neoadjuvant therapy in the treatment of cutaneous squamous cell carcinoma. Ann Plast Surg 92 (4S Suppl 2): S129-S131, 2024.
6. Hanna GJ, Ruiz ES, LeBoeuf NR, Thakuria M, Schmults CD, Decaprio JA and Silk AW: Real-world outcomes treating patients with advanced cutaneous squamous cell carcinoma with immune checkpoint inhibitors (CPI). Br J Cancer 123: 1535-1542, 2020.
7. Galambus J and Tsai KY: Molecular and immune targets in cutaneous squamous cell carcinoma. Mol Carcinog 62: 38-51, 2023.
8. Di Nardo L, Pellegrini C, Di Stefani A, Del Regno L, Sollena P, Piccerillo A, Longo C, Garbe C, Fargnoli MC and Peris K: Molecular genetics of cutaneous squamous cell carcinoma: Perspective for treatment strategies. J Eur Acad Dermatol Venereol 34: 932-941, 2020.
9. Thai AA, Lim AM, Solomon BJ and Rischin D: Biology and treatment advances in cutaneous squamous cell carcinoma. Cancers (Basel) 13: 5645, 2021.
10. Pham JP, Rodrigues A, Goldinger SM, Sim HW and Liu J: Epidermal growth factor receptor inhibitors in advanced cutaneous squamous cell carcinoma: A systematic review and meta-analysis. Exp Dermatol 33: e14978, 2024.
11. Colombo E, Gurizzan C, Ottini A, Caspani F, Bergamini C, Locati LD, Marchiselli C, Alberti A, Lorini L, Licitra LF, *et al*: The association of cemiplimab plus sonidegib for synchronous cutaneous squamous cell carcinoma and basal cell carcinoma of the head and neck: Two case reports. Front Oncol 13: 1111146, 2023.
12. London M and Gallo E: Epidermal growth factor receptor (EGFR) involvement in epithelial-derived cancers and its current antibody-based immunotherapies. Cell Biol Int 44: 1267-1282, 2020.
13. Cañueto J, Cardeñoso E, García JL, Santos-Briz Á, Castellanos-Martín A, Fernández-López E, Blanco Gómez A, Pérez-Losada J and Román-Curto C: Epidermal growth factor receptor expression is associated with poor outcome in cutaneous squamous cell carcinoma. Br J Dermatol 176: 1279-1287, 2017.
14. Sweeny L, Dean NR, Magnuson JS, Carroll WR, Helman EE, Hyde SO, Desmond RL and Rosenthal EL: EGFR expression in advanced head and neck cutaneous squamous cell carcinoma. Head Neck 34: 681-686, 2012.
15. Yang B, Zhang H, Dong L, Wang J and Yu N: Identification of PI3K/AKT/mTOR-related genes as diagnostic biomarkers for cutaneous squamous cell carcinoma. Biochem Biophys Rep 45: 102355, 2025.
16. Chang M, Samlowski W and Meoz R: Effectiveness and toxicity of cetuximab with concurrent RT in locally advanced cutaneous squamous cell skin cancer: A case series. Oncotarget 14: 709-718, 2023.
17. Riihilä P, Viiklepp K, Nissinen L, Farshchian M, Kallajoki M, Kivisaari A, Meri S, Peltonen J, Peltonen S and Kähäri VM: Tumour-cell-derived complement components C1r and C1s promote growth of cutaneous squamous cell carcinoma. Br J Dermatol 182: 658-670, 2020.
18. Zou DD, Sun YZ, Li XJ, Wu WJ, Xu D, He YT, Qi J, Tu Y, Tang Y, Tu YH, *et al*: Single-cell sequencing highlights heterogeneity and malignant progression in actinic keratosis and cutaneous squamous cell carcinoma. Elife 12: e85270, 2023.
19. Ji AL, Rubin AJ, Thrane K, Jiang S, Reynolds DL, Meyers RM, Guo MG, George BM, Mollbrink A, Bergenstråhle J, *et al*: Multimodal analysis of composition and spatial architecture in human squamous cell carcinoma. Cell 182: 497-514.e22, 2020.
20. Schütz S, Solé-Boldo L, Lucena-Porcel C, Hoffmann J, Brobeil A, Lonsdorf AS, Rodríguez-Paredes M and Lyko F: Functionally distinct cancer-associated fibroblast subpopulations establish a tumor promoting environment in squamous cell carcinoma. Nat Commun 14: 5413, 2023.
21. Li X, Zhao S, Bian X, Zhang L, Lu L, Pei S, Dong L, Shi W, Huang L, Zhang X, *et al*: Signatures of EMT, immunosuppression, and inflammation in primary and recurrent human cutaneous squamous cell carcinoma at single-cell resolution. Theranostics 12: 7532-7549, 2022.
22. Barrett T and Edgar R: Mining microarray data at NCBI's gene expression omnibus (GEO)*. Methods Mol Biol 338: 175-190, 2006.
23. Tian Q, Wang M, Mubeen F, Sundas A, Naz R, Hu X and Chen X: CDKN2A and matrix metalloproteinases: Key regulators of cellular senescence in squamous cell carcinoma. Am J Transl Res 17: 4573-4589, 2025.
24. O'Donnell BL, Johnston D, Bhatt A, Kardan Z, Stefan D, Bysice A, Sayedyahossein S, Dagnino L, Cecchini M, Loganathan SK, *et al*: Pannexin 1 and pannexin 3 differentially regulate the cancer cell properties of cutaneous squamous cell carcinoma. J Physiol 603: 4409-4432, 2025.
25. Stelzer G, Rosen N, Plaschkes I, Zimmerman S, Twik M, Fishilevich S, Stein TI, Nudel R, Lieder I, Mazor Y, *et al*: The GeneCards suite: From gene data mining to disease genome sequence analyses. Curr Protoc Bioinformatics 54: 1.30.1-1.30.33, 2016.
26. Sherman BT, Hao M, Qiu J, Jiao X, Baseler MW, Lane HC, Imamichi T and Chang W: DAVID: A web server for functional enrichment analysis and functional annotation of gene lists (2021 update). Nucleic Acids Res 50 (W1): W216-W221, 2022.
27. Kanehisa M: The KEGG database. Novartis Found Symp 247: 91-103, 119-128, 244-252, 2002.
28. Ashburner M, Ball CA, Blake JA, Botstein D, Butler H, Cherry JM, Davis AP, Dolinski K, Dwight SS, Eppig JT, *et al*: Gene ontology: Tool for the unification of biology. The gene ontology consortium. Nat Genet 25: 25-29, 2000.
29. Szklarczyk D, Gable AL, Nastou KC, Lyon D, Kirsch R, Pyysalo S, Doncheva NT, Legeay M, Fang T, Bork P, *et al*: The STRING database in 2021: Customizable protein-protein networks, and functional characterization of user-uploaded gene/measurement sets. Nucleic Acids Res 49 (D1): D605-D612, 2021.
30. Smoot ME, Ono K, Ruscheinski J, Wang PL and Ideker T: Cytoscape 2.8: New features for data integration and network visualization. Bioinformatics 27: 431-432, 2011.
31. Saito R, Smoot ME, Ono K, Ruscheinski J, Wang PL, Lotia S, Pico AR, Bader GD and Ideker T: A travel guide to Cytoscape plugins. Nat Methods 9: 1069-1076, 2012.
32. Chin CH, Chen SH, Wu HH L, Ho CW, Ko MT and Lin CY: cytoHubba: Identifying hub objects and sub-networks from complex interactome. BMC Syst Biol 8 (Suppl 4): S11, 2014.
33. Karumuri R, Shah D and Arnouk H: Cornulin as a potential novel biomarker for cutaneous squamous cell carcinoma. Cureus 14: e31694, 2022.
34. da Silva CN, Grassi TF, Miot HA and Espósito ACC: Expression of the aryl hydrocarbon receptor (AhR) in facial melasma skin compared to healthy perilesional skin. An Bras Dermatol 100: 501181, 2025.
35. Catalano M, Nozzoli F, De Logu F, Nassini R and Roviello G: Management approaches for high-risk cutaneous squamous cell carcinoma with perineural invasion: An updated review. Curr Treat Options Oncol 25: 1184-1192, 2024.
36. Winge MCG, Kellman LN, Guo K, Tang JY, Swetter SM, Aasi SZ, Sarin KY, Chang ALS and Khavari PA: Advances in cutaneous squamous cell carcinoma. Nat Rev Cancer 23: 430-449, 2023.
37. Venables ZC, Autier P, Nijsten T, Wong KF, Langan SM, Rous B, Broggio J, Harwood C, Henson K, Proby CM, *et al*: Nationwide incidence of metastatic cutaneous squamous cell carcinoma in England. JAMA Dermatol 155: 298-306, 2019.
38. Tokez S, Wakkee M, Kan W, Venables ZC, Mooyaart AL, Louwman M, Nijsten T and Hollestein LM: Cumulative incidence and disease-specific survival of metastatic cutaneous squamous cell carcinoma: A nationwide cancer registry study. J Am Acad Dermatol 86: 331-338, 2022.

39. Corchado-Cobos R, García-Sancha N, González-Sarmiento R, Pérez-Losada J and Cañueto J: Cutaneous squamous cell carcinoma: from biology to therapy. Int J Mol Sci 21: 2956, 2020.
40. Bailey P, Ridgway RA, Cammareri P, Treanor-Taylor M, Bailey UM, Schoenherr C, Bone M, Schreyer D, Purdie K, Thomson J, *et al*: Driver gene combinations dictate cutaneous squamous cell carcinoma disease continuum progression. Nat Commun 14: 5211, 2023.
41. Kim YS, Jung SH, Park YM, Park GS, Kim HS, Maeng LS and Chung YJ: Targeted deep sequencing reveals genomic alterations of actinic keratosis/cutaneous squamous cell carcinoma in situ and cutaneous squamous cell carcinoma. Exp Dermatol 32: 447-456, 2023.
42. Ke Y and Wang XJ: TGFβ signaling in photoaging and UV-induced skin cancer. J Invest Dermatol 141 (4S): S1104-S1110, 2021.
43. Ascierto PA and Schadendorf D: Update in the treatment of non-melanoma skin cancers: The use of PD-1 inhibitors in basal cell carcinoma and cutaneous squamous-cell carcinoma. J Immunother Cancer 10: e005082, 2022.
44. Anderson-Crannage M, Ascensión AM, Ibanez-Solé O, Zhu H, Schaefer E, Ottomanelli D, Hochberg B, Pan J, Luo W, Tian M, *et al*: Inflammation-mediated fibroblast activation and immune dysregulation in collagen VII-deficient skin. Front Immunol 14: 1211505, 2023.
45. Riihilä P, Nissinen L and Kähäri VM: Matrix metalloproteinases in keratinocyte carcinomas. Exp Dermatol 30: 50-61, 2021.
46. Ahmady S, Jansen MHE, Nelemans PJ, Kessels JPHM, Arits AHMM, de Rooij MJM, Essers BAB, Quaedvlieg PJF, Kelleners-Smeets NWJ and Mosterd K: Risk of invasive cutaneous squamous cell carcinoma after different treatments for actinic keratosis: A secondary analysis of a randomized clinical trial. JAMA Dermatol 158: 634-640, 2022.
47. Hareendran S, Albraidy B, Yang X, Liu A, Breggia A, Chen CC and Loh YP: Exosomal carboxypeptidase E (CPE) and CPE-shRNA-loaded exosomes regulate metastatic phenotype of tumor cells. Int J Mol Sci 23: 3113, 2022.
48. Fuchs A and Marmur E: The kinetics of skin cancer: Progression of actinic keratosis to squamous cell carcinoma. Dermatol Surg 33: 1099-1101, 2007.
49. Thind AS, Ashford B, Strbenac D, Mitchell J, Lee J, Mueller SA, Minaei E, Perry JR, Ch'ng S, Iyer NG, *et al*: Whole genome analysis reveals the genomic complexity in metastatic cutaneous squamous cell carcinoma. Front Oncol 12: 919118, 2022.
50. Lu H, Peng Z, Zheng Z, Li C, Wang Y, Liang L, Chen Y and Zeng K: Blocking the ATR-SerRS-VEGFA pathway targets angiogenesis for UV-induced cutaneous squamous cell carcinoma. Mol Carcinogs 63: 1160-1173, 2024.
51. Ding Y, Yi J, Wang J and Sun Z: Interleukin-1 receptor antagonist: A promising cytokine against human squamous cell carcinomas. Heliyon 9: e14960, 2023.
52. Powers JM, Murphy G, Ralph N, O'Gorman SM and Murphy JEJ: Polypharmacy and sun exposure: Implications for mitochondrial DNA deletions in skin. J Photochem Photobiol B 173: 397-403, 2017.
53. Khalaf K, Hana D, Chou JT, Singh C, Mackiewicz A and Kaczmarek M: Aspects of the tumor microenvironment involved in immune resistance and drug resistance. Front Immunol 12: 656364, 2021.
54. Simon T and Salhia B: Cancer-associated fibroblast subpopulations with diverse and dynamic roles in the tumor microenvironment. Mol Cancer Res 20: 183-192, 2022.
55. Mao X, Xu J, Wang W, Liang C, Hua J, Liu J, Zhang B, Meng Q, Yu X and Shi S: Crosstalk between cancer-associated fibroblasts and immune cells in the tumor microenvironment: New findings and future perspectives. Mol Cancer 20: 131, 2021.
56. Chen J, Dang Y, Feng W, Qiao C, Liu D, Zhang T, Wang Y, Tian D, Fan D, Nie Y, *et al*: SOX18 promotes gastric cancer metastasis through transactivating MCAM and CCL7. Oncogene 39: 5536-5552, 2020.
57. An Y, Wei N, Cheng X, Li Y, Liu H, Wang J, Xu Z, Sun Z and Zhang X: MCAM abnormal expression and clinical outcome associations are highly cancer dependent as revealed through pan-cancer analysis. Brief Bioinform 21: 709-718, 2020.
58. Pang Y, Maxwell E, Sindrewicz-Goral P, Shapanis A, Li S, Morgan M and Yu LG: Galectin-3 is a natural binding ligand of MCAM (CD146, MUC18) in melanoma cells and their interaction promotes melanoma progression. Biomolecules 12: 1451, 2022.
59. Kobayashi H, Gieniec KA, Lannagan TRM, Wang T, Asai N, Mizutani Y, Iida T, Ando R, Thomas EM, Sakai A, *et al*: The origin and contribution of cancer-associated fibroblasts in colorectal carcinogenesis. Gastroenterology 162: 890-906, 2022.
60. Yang W, Zhang S, Li T, Zhou Z and Pan J: Single-cell analysis reveals that cancer-associated fibroblasts stimulate oral squamous cell carcinoma invasion via the TGF-β/Smad pathway. Acta Biochim Biophys Sin (Shanghai) 55: 262-273, 2022.
61. Jain S, Rick JW, Joshi RS, Beniwal A, Spatz J, Gill S, Chang AC, Choudhary N, Nguyen AT, Sudhir S, *et al*: Single-cell RNA sequencing and spatial transcriptomics reveal cancer-associated fibroblasts in glioblastoma with protumoral effects. J Clin Invest 133: e147087, 2023.
62. Wei X, Lou H, Zhou D, Jia Y, Li H, Huang Q, Ma J, Yang Z, Sun C, Meng Y, *et al*: TAGLN mediated stiffness-regulated ovarian cancer progression via RhoA/ROCK pathway. J Exp Clin Cancer Res 40: 292, 2021.
63. Sarubo M, Mouri Y, Moromizato A, Yamada A, Jin S, Shao W, Hagita H, Miyoshi K and Kudo Y: Involvement of TGFBI-TAGLN axis in cancer stem cell property of head and neck squamous cell carcinoma. Sci Rep 14: 6767, 2024.
64. Li H, Song C, Zhang Y, Liu G, Mi H, Li Y, Chen Z, Ma X, Zhang P, Cheng L, *et al*: Transgelin promotes glioblastoma stem cell hypoxic responses and maintenance through p53 acetylation. Adv Sci (Weinh) 11: e2305620, 2024.
65. Ganier C, Mazin P, Herrera-Oropeza G, Du-Harpur X, Blakeley M, Gabriel J, Predeus AV, Cakir B, Prete M, Harun N, *et al*: Multiscale spatial mapping of cell populations across anatomical sites in healthy human skin and basal cell carcinoma. Proc Natl Acad Sci USA 121: e2313326120, 2024.
66. Wu X, Lu W, Zhang W, Zhang D, Mei H, Zhang M, Cui Y and Zhuo Z: Integrated analysis of single-cell RNA-seq and bulk RNA-seq unravels the heterogeneity of cancer-associated fibroblasts in TNBC. Aging (Albany NY) 15: 12674-12697, 2023.
67. Primac I, Maquoi E, Blacher S, Heljasvaara R, Van Deun J, Smeland HY, Canale A, Louis T, Stuhr L, Sounni NE, *et al*: Stromal integrin α11 regulates PDGFR-β signaling and promotes breast cancer progression. J Clin Invest 129: 4609-4628, 2019.
68. Wu SZ, Roden DL, Wang C, Holliday H, Harvey K, Cazet AS, Murphy KJ, Pereira B, Al-Eryani G, Bartonicek N, *et al*: Stromal cell diversity associated with immune evasion in human triple-negative breast cancer. EMBO J 39: e104063, 2020.

Copyright © 2026 Deng et al. This work is licensed under a Creative Commons Attribution-NonCommercial-NoDerivatives 4.0 International (CC BY-NC-ND 4.0) License.